

Rheological Properties of Hydrolyzed Polyacrylonitrile-Grafted Cellulose

A-T. CAO-THI and A. A. ROBERTSON, *Pulp and Paper Research Institute of Canada and Department of Chemistry, McGill University, Montreal, Quebec, Canada, H3A 2A7*

Synopsis

The rheological properties of aqueous dispersions of hydrolyzed polyacrylonitrile-grafted cellulose (H-CPAN) have been investigated. The experimental results are consistent with the idea that the elementary particle is a rigid cellulose protofibril stabilized in suspension by associated polyelectrolyte side chains (polyacrylamide-polyacrylic acid copolymer grafts). The behavior of intrinsic viscosity with electrolyte concentration, the concentration dependence and shear dependence of the viscosity and of the steady-state and dynamic shear moduli are qualitatively explained on this basis.

INTRODUCTION

Polyacrylonitrile grafts may be polymerized onto native cellulose fibers and subsequently converted by alkaline hydrolysis to a copolymer of sodium polyacrylate and polyacrylamide. This treatment results in fibers that are highly swollen, and, in this state, they may be dispersed by mechanical treatment into a suspension of elementary particles. The preparation, treatment, and an initial rheological study have been reported in earlier publications.^{1,2} The properties of this material have been compared with those of an analogous product based on starch by Taylor and Bagley,³ who have suggested the abbreviations H-CPAN and H-SPAN for the two products.

Examination of the dispersed material, by electron microscopy, reveals rodlike elements with lengths greater than the field diameter and with a lateral dimension of the order of 5 nm (Fig. 1). These are assumed to be crystalline cellulose protofibrils. For reasons set forth previously,¹ the rheological behavior of the suspension is attributed primarily to the stiffness of these rodlike particles, whose dispersion is maintained by the steric and electrostatic stabilization provided by the polyelectrolyte grafts.

This paper reports rheological studies of these suspensions, and an attempt is made to interpret the results in terms of the interactions of stiff rodlike particles.

This investigation has been pursued by looking first at the properties of the elementary particles by intrinsic viscosity measurements in an Ubbelohde viscometer. Then the dependence of viscosity on concentration is followed progressively in the capillary viscometer, a concentric cylinder viscometer (Epprecht), and a cone-and-plate viscometer (I-Mass Mechanical Spectrometer). The mechanical spectrometer is used further to establish the elastic moduli of the suspension at representative concentrations through the measurement of normal shear stresses and oscillatory shear behavior.

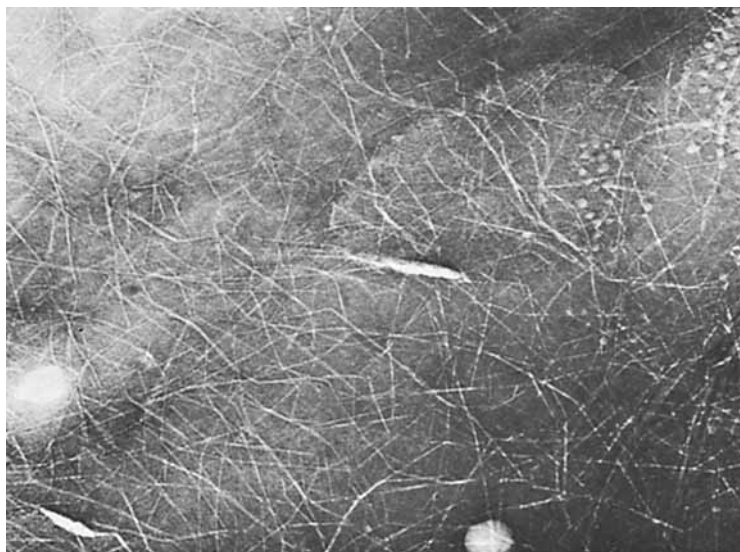


Fig. 1. Electron micrograph of a film obtained by drying a colloidal suspension of H-CPAN. Magnification $\times 825,000$.

RESULTS AND DISCUSSION

Intrinsic Viscosity

Reduced viscosity plots for dilute suspensions of the hydrolyzed polyacrylonitrile grafted cellulose (H-CPAN) are reproduced in Figure 2 at several electrolyte concentrations. Intrinsic viscosities, obtained by the extrapolations, are given in Table I.

It is assumed that the intrinsic viscosity is determined by the shape of the particle which is seen to be rodlike. Neither the real nor the effective length of the rods is readily determined from the electron microscope images because of

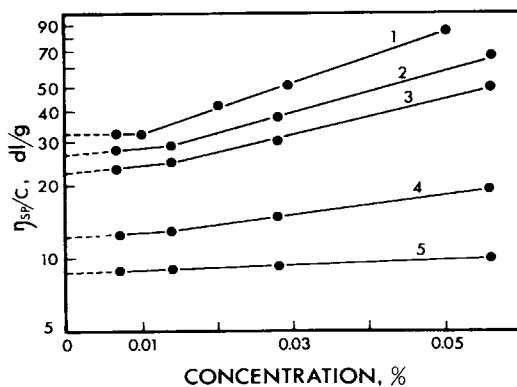


Fig. 2. Reduced specific viscosity as a function of concentration for dilute H-CPAN suspensions at the following electrolyte concentrations (NaCl):

Curve	1	2	3	4	5
Concn (mM)	0	2.6	5.6	48	90

TABLE I
 Intrinsic Viscosity and Particle Dimensions

Ionic strength μ (mmol/L)	Intrinsic viscosity $[\eta]$ (dL/g)	Expansion factor α	Axis ratio r	Specific volume V_{sp} (cc/g)
0	32.2	24	5.4	480
2.6	26.5	20	6.5	330
5.6	22.5	16	8.1	215
48	12.2	4.6	28	18
90	8.7	1.5	87	1.9

the difficulty of end-to-end scanning and the occurrence of abrupt bends or kinks in the protofibrils. The change in intrinsic viscosity with electrolyte concentration is attributed to the extension of the grafted polyelectrolyte chains. Thus the effective axis ratio of the particle is believed to change as a result of changes in the cross-sectional dimension. Since the length dimension is expected to be unchanged by electrolyte concentration or dilution, the viscosity should be less sensitive to these variables than would be the case for flexible polyelectrolytes.

The data have been examined by relating them to Simha's treatment of the viscosity behavior of a dilute suspension of randomly oriented ellipsoids of large axis ratio.⁴ His result may be written as

$$[\eta] = \frac{V_{sp}}{100} \left[\frac{14}{15} + \frac{r^2}{15 (\ln 2r - 1.5)} + \frac{r^2}{5 (\ln 2r - 0.5)} \right] \quad (1)$$

where r = the axis ratio of the particles and V_{sp} = the specific volume of the particles.

If it is assumed that the H-CPAN particles have a fixed length l and a cross-sectional dimension a and that the effective cross section is increased by an expansion coefficient α due to the effective specific volume of the stabilizing polyelectrolyte chains, then, assuming a density ρ of the cellulose rod plus polymer, the hydrodynamic specific volume of the particle is $V_{sp} = \alpha^2/\rho$ cc/g cellulose and the axis ratio is $l/\alpha a$.

Equation (1) may then be rewritten in terms of l , α , and a instead of V_{sp} and r .

The following assumptions are now made. The basic lateral dimension of the protofibril is 3.5 nm,⁵ and this is increased to 5.75 nm by the presence of PAAc—PAAm at a graft level of 112%, distributed as side chains along the protofibril length and having the density of bulk polymer (~ 1.0). The density of cellulose is taken as 1.5 and the density of the particles calculated on this basis is 1.19. The suspension is assumed to be monodisperse and to consist of particles having a constant length of 750 nm. This value for l is only selected to provide reasonable values for α and does not represent a measured value.

If these assumed values for l , a , and α are introduced into eq. (1), we obtain

$$[\eta] = 7.8 \times 10^{-3} \alpha^2 + \frac{9.4}{4.0 - \ln \alpha} + \frac{28.2}{5.0 - \ln \alpha} \quad (2)$$

Solution of this equation, for the experimental values of $[\eta]$, provides the values of α , axis ratio $r (= l/\alpha z)$, and $V_{sp} (= \alpha^2/\rho)$ that are shown in Table I.

The values obtained are speculative but not unreasonable. In view of the assumptions made, they are only illustrative and have limited quantitative significance. They are, however, self-consistent and are presented to suggest the possible influence of the addition of electrolyte on the degree to which the polyelectrolyte side chains are extended. At low ionic strength the chains are expected to be fully extended, as has been demonstrated by viscosity and optical measurements of homopolymers of polyacrylic acid^{6,7} and other polyelectrolytes. At higher ionic strengths, the polyelectrolyte chains are believed to be increasingly coiled, and the decreasing apparent specific volume of the H-CPAN particles reflects this trend. If salt is added in excess of 0.1 mol/L, the H-CPAN suspension becomes unstable and coagulates.

The visualization of H-CPAN particles having hydrodynamic properties equivalent to a model with assignable dimensions and volume provides the basis for considering the behavior of suspensions of these particles at finite concentrations.

The dependence of intrinsic viscosity on electrolyte concentration, recorded in Figure 2 and Table I, is shown in Figure 3 to have an inverse relationship. The logarithmic plot at finite electrolyte concentrations has varying negative slope with a mean value of about -0.3 . This may be compared with the invariability of the intrinsic viscosity of DNA—a rigid rodlike macromolecule—over an extended range of electrolyte concentrations⁸ and the dependence of intrinsic viscosity on the inverse 0.5 power of electrolyte concentration frequently observed for flexible polyelectrolytes.^{9,10} The intermediate concentration dependence observed here is appropriate for a rigid rod of fixed length but variable cross section and axis ratio.

Concentration Dependence

A composite viscosity–concentration graph, plotted logarithmically, is shown in Figure 4 and includes representative data from the capillary, concentric cylinder, and cone-and-plate viscometers at low, medium, and high viscosities, respectively. The shear rate was varied from 2.5 s^{-1} to 250 s^{-1} for the more viscous

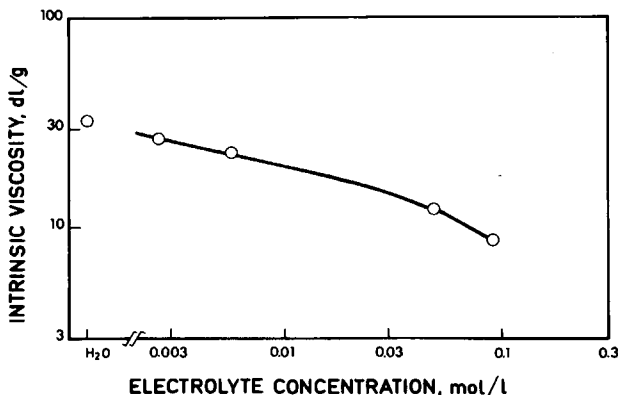


Fig. 3. Intrinsic viscosity as a function of electrolyte concentration.

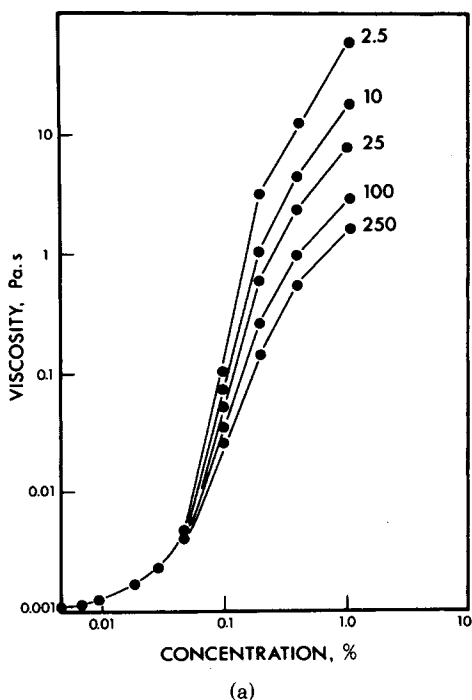


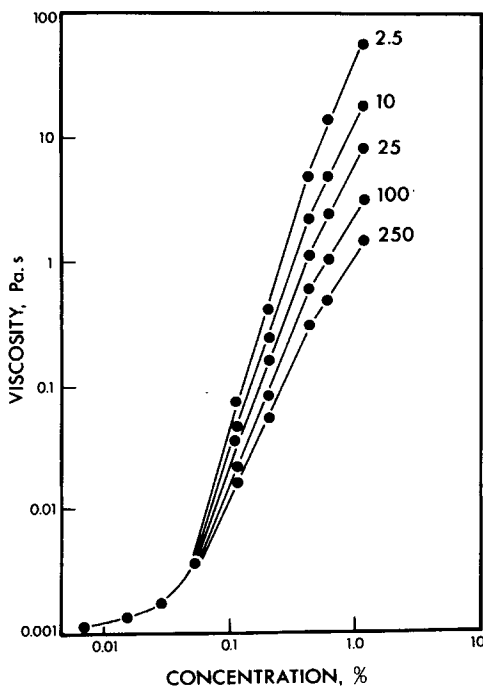
Fig. 4. Concentration dependence of apparent viscosity measured at different shear rates as shown (s^{-1}). (a) Water dilution; (b) isoionic dilution.

suspensions, but the shear dependence at concentrations below 0.05 g/dL was relatively small and was regarded as approximating Newtonian behavior. Concentrations were obtained by dilution from 1.12 g/dL stock suspension by either (1) water or (2) isoionic dilution with 0.0056M NaCl.

The changing dependence of the specific viscosity on concentration with increasing concentration may be followed (Fig. 5) by the derivative of the curves to give the exponent of the concentration C . The exponent is seen to rise from a fractional value at the lowest dilution through a maximum before falling toward unity.

Several observations may be made on the concentration dependence. It has been shown by Mason¹¹ that there should be a critical concentration of rodlike particles at which the volume swept out by rods orbiting in shear equals the volume of the suspension. Above this, the increased incidence of collision and interaction leads to an increase of viscosity. The critical concentration for particles having the r and V_{sp} values shown in Table I is about 0.01% by weight. This value is consistent with the curves in Figures 2 and 4, and the viscosity increases rapidly once this concentration is exceeded.

The increase in concentration dependence above the critical concentration is such that the exponent E (Fig. 5) reaches 4 or 5 at the lower shear rates (2.5 s^{-1}). The increase is logically attributed to particle interactions and transient structures in increasingly crowded systems. The theoretical basis to account for viscosity behavior in intermediate concentration ranges is not well developed; but viscosity dependence on concentration to the fifth power has been cited by Ferry¹² for polymer solutions, and Hayashi¹³ has developed expressions based



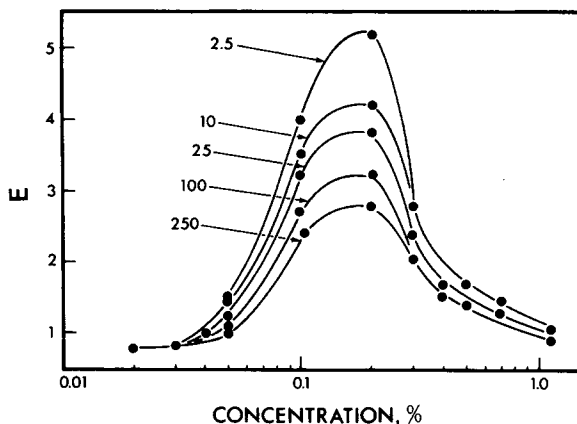
(b)

Fig. 4. (Continued from previous page.)

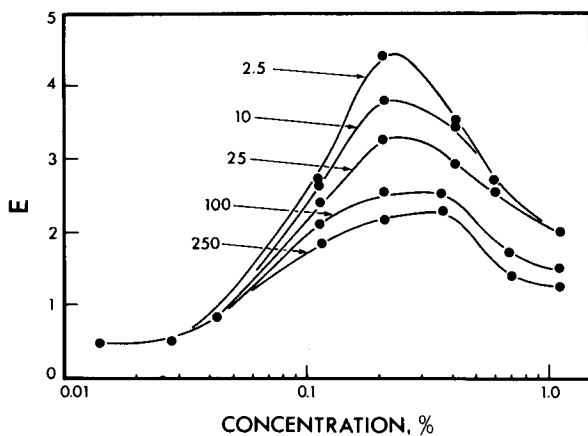
on a network model that predict a dependence of viscosity on concentration to the power of 3.5 at moderate concentrations and to a power of 6 at high concentrations. In making these comparisons, it must be recognized that the experimental apparent viscosities are shear-dependent and are being determined at a finite shear rate while predictions of concentration dependence usually refer to zero-shear conditions.

The decreasing concentration dependence at higher concentrations is at first sight unexpected and suggests a changing flow mechanism. The phenomenon arises as the volume fraction of the particles, based on the specific volumes established by intrinsic viscosity (Table I), approaches unity. This corresponds to approximately 0.2% and 0.5% for water and isoionic dilution, respectively. In suspensions approaching and exceeding these concentrations, particles are crowded or compressed, and the possibility of motion of the particles depends on their deformability and further compression.

Decreases in concentration dependence with increasing concentration are not often encountered in the literature. Bagley and Taylor¹⁴ have described an analogous system. Although the system is crowded, the lateral compressibility of the individual particles depends on the deformability of extended polyelectrolyte chains, and these may offer little resistance. Bagley and Taylor¹⁴ imply that the low concentration dependence in H-SPAN suspensions is related to the condition that, over a range of concentrations, the volume fraction of particles approximates unity, corresponding to compressed swollen particles that expand with dilution. Dilution below some critical point results in free volume developing between the particles, and viscosity then decreases steeply with further



(a)



(b)

Fig. 5. The change in concentration dependence of apparent viscosity with concentration is obtained from the slopes of the curves in Figure 3. The ordinate E is $\Delta \log \eta_p / \Delta \log C$. Five shear rates (s^{-1}) are shown for (a) water dilution and (b) isoionic dilution.

dilution. Other possibilities to consider are the development of wall slip,¹⁵ slip planes within the fluid, or enhanced particle orientation during flow.

On the basis of steady-state viscosity vs. concentration, it is therefore possible to infer several stages of interaction and structure development with concentration, beginning with independent motion of the particles but with increasing particle collision and interaction as the concentration increases to the point that interaction and structure formation lead to gel-like behavior. The formation of structures results in pronounced thixotropy and pseudoplasticity.

Shear Rate Dependence

Viscosity

The apparent viscosity is shown as a function of shear rate for several concentrations of H-CPAN in Figure 6.

Over much of the experimental range, the material is pseudoplastic, that is,

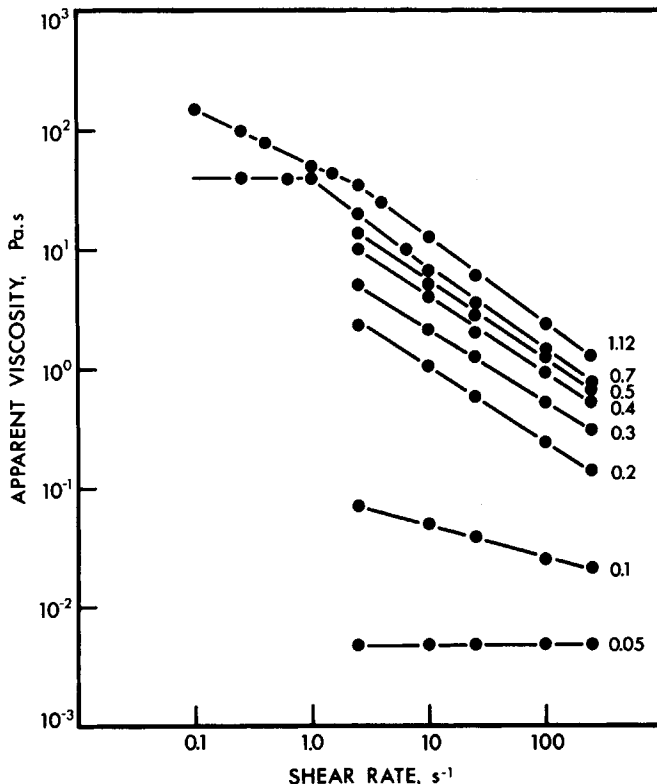


Fig. 6. Dependence of apparent viscosity on shear rate for suspensions having concentrations between 0.05% and 1.12%.

the viscosity decreases with increasing rate of shear. Moreover, the behavior follows the "power law" above a critical shear rate and

$$\eta_p = K \cdot \dot{\gamma}^{n-1}$$

where η_p is the apparent viscosity, K and n are constants, and $\dot{\gamma}$ is the shear rate. When a material is Newtonian, the flow index $n = 1$ and $K = \eta_p$; when the material is dilatant, $n > 1$.

Here the H-CPAN dispersions are pseudoplastic and the flow index $n < 1$. Measurements of the slope, taken from Figure 6 in the power-law region, provide the typical values of n listed in Table II. The flow index remains fairly constant at 0.33 for concentrations above 0.5% but increases at lower concentrations. Below 0.05% the viscosity is independent of shear and $n \sim 1$ over the range of shear rates investigated.

As the shear rate decreases from the power-law region, the flow index increases, and this effect has been investigated from H-CPAN concentrations of 0.7% and 1.12%. In the experimentally accessible region of the 0.7% suspension, the viscosity levels off to a Newtonian plateau when $\dot{\gamma} < 1 \text{ s}^{-1}$ and n becomes unity. On the other hand, although the 1.12% material shows an increase in n with decreasing shear rate, a plateau is not reached.

It is of interest to compare this result with the recorded or predicted behavior of other suspensions. The shear-rate independence of viscosity at low shear

TABLE II
Shear-Rate Dependence of Viscosity

Concn (%)	Flow index n
1.12	0.30
0.8	0.33
0.7	0.33
0.5	0.33
0.4	0.37
0.2	0.37
0.1	0.72
0.05	1.0

rates, followed by an increasing dependence on shear at increasing shear rates, is frequently observed,^{16,17} although shear dependence at various concentrations is not available for many systems.

Comparative curves have been published by Graessley¹⁶ for polymer solutions. His compilation of work from several sources has shown that for these systems the flow index in the power-law region decreases with increase in concentration normalized as a "coil overlap parameter" or "pervaded volume" $C[\eta]$. The flow index levels out with values between 0.4 and 0.3 when the product of the concentration and the intrinsic viscosity, $C[\eta]$, reached a value of 15 or 20. The behavior of H-CPAN may be compared with that of polymer solutions by noting that $C[\eta] = 15$ at concentrations of 0.47% and 0.67% for dilutions with water and isoionic solutions, respectively, and the flow index for higher concentrations is near 0.33.

This concept of a pervaded volume parameter $C[\eta]$ is similar to the identification made earlier of the concentration at which the particle partial volume becomes unity, $CV_{sp} = 1$. The values of $C = 0.2\%$ and 0.5% , respectively, correlated with the point at which the concentration dependence of viscosity began to decrease (Fig. 5). The two criteria reflect different stages of the transition from the behavior at low concentrations (high dependence of viscosity on concentration and low dependence on shear) to the behavior at high concentrations (lower dependence on concentration and a higher constant dependence on shear).

Typical shear dependent behavior is illustrated schematically in Figure 7. The curves are drawn to be representative of data in the literature for polymer solutions. See, for example, Graessley¹⁶ and Blanks.¹⁷ The figure summarizes the interrelationships of concentration, shear rate, and apparent viscosity. The features of interest are the zero-shear viscosity and its associated Newtonian plateau, the transition from Newtonian behavior to shear-thinning at decreasing shear rates as the concentration is higher, and the trend to a uniform power-law dependence at higher shear rates.

These summarized effects are well known and have been treated from different viewpoints by different authors. The concentration dependence of the zero shear viscosity is predicted in some measure by the entanglement theories of Lodge,¹⁸ but the explanation of the inception and development of shear-thinning require developments such as those proposed by Graessley,¹⁶ Bird and Carreau,¹⁹ and Meister.²⁰ These theories or methods of analysis are consistent with the schematic curves shown and have been fitted to the experimental data of Blanks.¹⁷

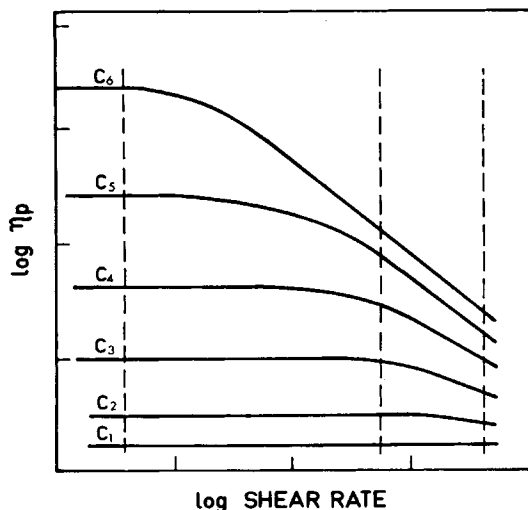


Fig. 7. Shear rate dependence of polymer solutions and suspensions at different concentrations. Schematic only.

The assumptions made by Lodge, Graessley, Bird, or Meister and found applicable to polymer solutions cannot be valid except in a very qualitative way in a suspension of relatively rigid rods. However, many of the features of the polymer solution behavior are observed with H-CPAN and are to be attributed to particle interactions. In Figure 7 the concentration dependence is seen to be different, depending on the rate of shear at which the viscosity measurements are made, and is greatest at the lowest shear rates and least at high shear. In the transition region, there are shear rates at which Newtonian behavior at low concentration coexists with shear-thinning at high concentration. This situation results in decreasing concentration dependence of apparent viscosities as concentration increases at these shear rates.

A consideration of Figure 6 suggests that the H-CPAN system being studied lies largely in this transition region and that the decrease in concentration dependence of higher concentrations shown in Figure 4 is consistent with a relatively greater shear-thinning effect at the higher concentrations. The effect therefore may not be peculiar to H-CPAN suspensions but may be a manifestation of a more general phenomenon in the shear properties of suspensions or solutions involving structures.

Figure 6 shows similarities with the idealized curves in Figure 7, but the Newtonian plateau is not adequately shown at low shear rates, although these are suggested at the two highest concentrations. The persistence of the constant flow index to lower shear rates is also illustrated in Figure 8, where the behavior of H-CPAN is compared with two polymer solutions that have been carefully studied: Separan (polyacrylamide-polyacrylic acid copolymer)¹⁷ and hydroxyethyl cellulose.¹⁹ The comparison is effected by multiplying the polymer solution viscosity data by a factor of 10. It is thus seen that the flow index for H-CPAN is less affected by shear rate than that of polymer solutions. At the same time, at similar concentrations, the rodlike particles give an apparent viscosity an order of magnitude higher.

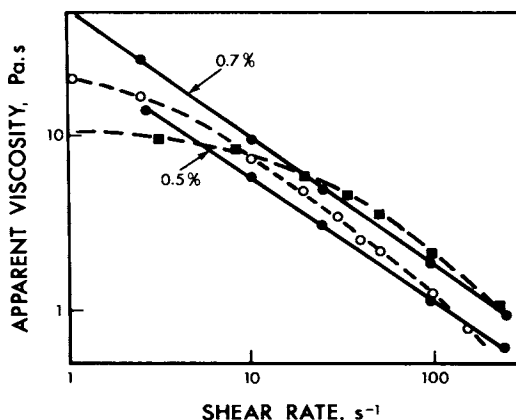


Fig. 8. The shear-rate dependence of H-CPAN suspension at 0.5% and 0.7% concentration (isoionic dilution) are compared with data from the literature: (O) 0.5% Separan solution¹⁷; (■) 0.9% hydroxyethyl cellulose.¹⁹ The literature viscosity data have been multiplied by 10 to make them comparable to H-CPAN.

Viscoelasticity

The cone-and-plate viscometer (I-mass mechanical spectrometer) was used to determine the viscosity at higher concentrations. The experimental results under steady shear provide not only the torque τ_{12} , by which the viscosity is measured, but also the normal force difference, $p_{11} - p_{22}$. These data may be used to calculate

- (a) the apparent viscosity

$$\eta_p = \tau_{12}/\dot{\gamma}$$

- (b) the normal stress difference function

$$\theta = (p_{11} - p_{22})/\dot{\gamma}^2$$

- (c) the apparent shear modulus

$$G = 2\tau_{12}^2/(p_{11} - p_{22}).$$

Plots of η_p , θ , and G as a function of $\dot{\gamma}$ are shown in Figures 8, 9, and 10, respectively, for higher suspension concentrations. At lower concentrations the measurements of normal stresses were unreliable and were not recorded.

The slope of the normal stress function θ is constant for concentrations of 0.5%, 0.7%, and 1.12%. The slope is compared with that for a Separan solution,¹⁷ which has been shown to conform to predictions made from the Bird-Carreau¹⁹ and Meister²⁰ models. Again the data relating to the polymer solution (0.5%) has been increased by a factor of 10 to permit the comparison. The extended linear behavior of the H-CPAN with a slope predicted for model polymer solutions is noted.

The shear moduli G , in general, increase moderately with concentration and shear rate, as shown in Figure 10. The data reveal a plateau reminiscent of the plateau obtained in measuring the moduli of a rubber at varying shear rate and frequency. A behavior suggests the presence of elastically deformable transient structures formed by interacting particles during shear.

The dynamic moduli of the suspensions were determined using the eccen-

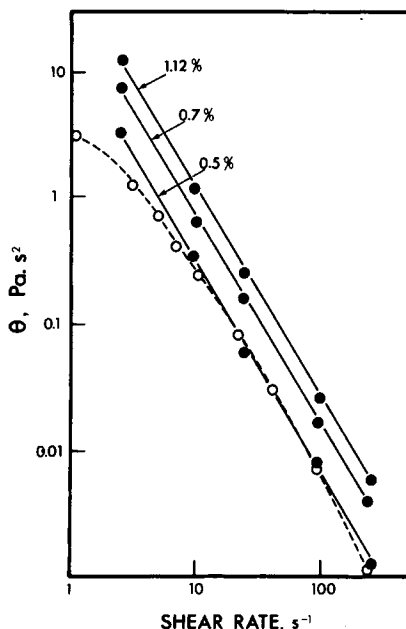


Fig. 9. The shear-rate dependence of θ for H-CPAN suspensions of 0.5%, 0.7%, and 1.12% concentrations is compared with the predictions of the Byrd and Carreau¹⁹ and Meister²⁰ models for Separan solutions.¹⁷ The literature viscosity data are multiplied by 10 to make them comparable to H-CPAN.

tric-rotating-disc mode²¹ of the mechanical spectrometer. This enabled the observation of the storage and loss moduli, G' and G'' , as a function of concentration and shear rate (frequency at a shear-strain amplitude of 0.5). The results for 0.5% concentrations are plotted in Figure 11.

It may be noted that the two dynamic moduli are of a similar magnitude as G , calculated from $p_{11} - p_{22}$, and that they also tend to a plateau value at low shear rates. The values of G , G' , and G'' essentially fall within a half a decade ($10^2 - 5 \cdot 10^2$ Pa) when the frequency varies over 3.5 decades. Detailed interpretation is not possible, but the behavior may be compared, for example, with the tests of the Kirkwood-Auer theory by Tschoegl and Ferry,²² using poly-(benzyl-*L*-glutamate). That system shows a less defined plateau because of its low concentration, but some similarity in the relative behavior of G' and G'' is noted. A similarity in behavior may also be seen²³) in the test of theory of Marvin and Oser using polyisobutylene and the test of the theory of Chompff and Prins with poly(*n*-octyl-methacrylate). These undiluted polymers provide more extended plateaus but again the interrelationships of G' and G'' are somewhat similar.

Thus, the behavior H-CPAN dispersions is comparable qualitatively with systems in which the behavior is attributed to entanglement coupling. Although it must be assumed that the particle interaction is quite different, the existence of similar viscoelastic behavior argues for interpretation in terms of deformable structures.

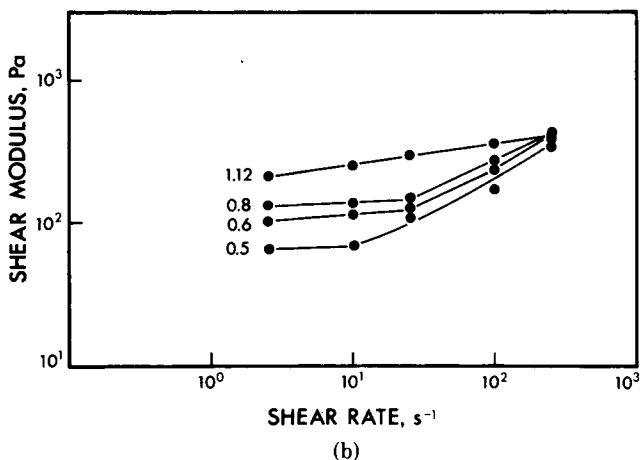
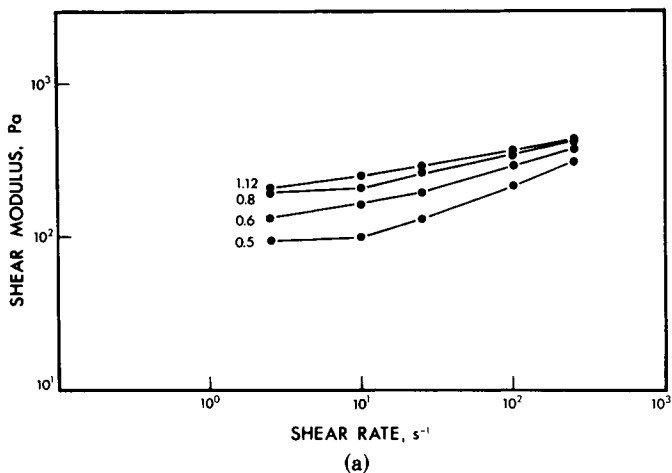


Fig. 10. Shear rate dependence of the shear modulus G for different suspension concentrations (wt %) as shown. (a) Water dilution; (b) isoionic dilution.

CONCLUDING REMARKS

Within the limits of the experimental techniques accessible to us, the results obtained for H-CPAN show that the rheological behavior differentiates fairly clearly low and high concentration regions. These are roughly indicated by the criteria that the product of concentration and hydrodynamic volume (CV_{sp}) of the particles is greater or less than unity or that the product of the concentration and intrinsic viscosity ($C[\eta]$) is greater or less than 15.

Above these critical concentrations (0.2–0.5% and 0.5–0.7% for water dilution and isoionic dilution, respectively), the concentration dependence of the apparent viscosity decreases, an elastic modulus that is insensitive to shear and concentration is measured, and the shear-rate dependence of apparent viscosity becomes independent of concentration ($n \sim 0.3$).

This behavior of the H-CPAN suspensions conforms, at least qualitatively, to experience with polymer solutions. It has not yet been possible to define any behavior directly attributable to the assumed particle stiffness other than that

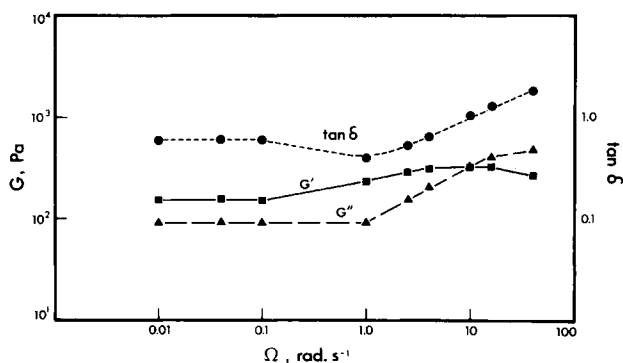


Fig. 11. Dynamic storage modulus G' , loss modulus G'' , and $\tan \delta$ for a 1.12% H-CPAN suspension vs. frequency.

the viscosity and normal shear stress are greater at a given concentration over molecularly dispersed polymers and that the dependence of intrinsic viscosity on electrolyte concentrations is less than is usually observed for flexible polyelectrolytes.

The potential of H-CPAN as a material for investigating rheological principles can be further realized by control, for example, of the particle length by mechanical or chemical treatment, of the cross section by control of the grafting, of the interactions by pH or ionic strength, and of the response by extending the range of experimental testing.

References

1. P. Lepoutre and A. A. Robertson, *Tappi*, **57**, 87 (1974).
2. J. W. Adams and A. H. Tilloson, U.S. Pat. 3,682,586 (1972).
3. N. W. Taylor and E. G. Bagley, *J. Appl. Polym. Sci.*, **21**, 1607 (1977).
4. H. O. Frisch and R. Simha, in *Rheology*, F. R. Eirich, Ed., Academic, New York, 1956, Vol. 1, Chap. 14.
5. R. St. J. Manley, *J. Polym. Sci., A-2*, **9**, 1025 (1971).
6. A. Oth and P. Dobry, *J. Phys. Chem.*, **56**, 43 (1952).
7. A. Katchalsky and H. J. Eisenberg, *Polym. Sci.*, **6**(2), 145 (1951).
8. R. A. Cox, *J. Polym. Sci.*, **47**, 411 (1960).
9. M. J. Fixman, *J. Chem. Phys.*, **41**, 3772 (1964).
10. H. W. Chien and A. Isihara, *J. Polym. Sci., Polym. Phys. Ed.*, **14**, 1015 (1976).
11. S. G. Mason, *Pulp Paper Mag. Can.*, **51**(5), 93 (1950).
12. J. D. Ferry, *Viscoelastic Properties of Polymers*, 2nd ed., Wiley, New York, 1970, p. 282.
13. S. Hayashi, *Proceedings of the Fifth International Congress on Rheology*, University of Tokyo Press, Tokyo, 1970, Vol. 4, p. 179.
14. N. W. Taylor and E. R. Bagley, *J. Polym. Sci.*, **13**, 1133 (1975).
15. H. L. Goldsmith and S. G. Mason, in *Rheology*, F. R. Eirich, Ed., Academic, New York, 1967, Vol. 4, Chap. 2.
16. W. W. Graessley, *Adv. Polym. Sci.*, **16**, (1974).
17. R. F. Blanks, H. C. Park, D. R. Patel, and M. C. Hawley, *Polym. Eng. Sci.*, **14**, 16 (1974).
18. A. S. Lodge, *Elastic Liquids*, Academic, New York, 1964.
19. B. R. Bird and P. J. Carreau, *Chem. Eng. Sci.*, **23**, 427 (1968).
20. B. J. Meister, *Trans. Soc. Rheol.*, **15**(1), 63 (1971).
21. C. Macosko and J. M. Starita, *Soc. Plast. Eng. J.*, **27**, 38 (1971).
22. N. W. Tschoegl and J. D. Ferry, *J. Am. Chem. Soc.*, **86**, 1474 (1964).
23. Ref. 12, p. 545.

Received July 17, 1981

Accepted November 23, 1981